Desalination and Water Treatment
www.deswater.com

doi:10.5004/dwt.2017.20648

72 (2017) 300–307
April

Graphene oxide cross-linked chitosan nanocomposite adsorbents for the removal of Cr (VI) from aqueous environments

Lirui Wu[a], Ziyi Qin[a], Fei Yu[b,c,*], Jie Ma[b,*]

[a]*School of Mechanical Engineering, Tongji University, 1239 Siping Road, Shanghai 200092, China*
[b]*State Key Laboratory of Pollution Control and Resource Reuse, School of Environmental Science and Engineering, Tongji University, 1239 Siping Road, Shanghai 200092, China, Tel. 86-21-65981831, email: jma@tongji.edu.cn (J. Ma)*
[c]*School of Chemical and Environmental Engineering, Shanghai Institute of Technology, 100 Hai Quan Road, Shanghai 201418, China, Tel. 86-21-60873182, email: fyu@vip.163.com (F. Yu)*

Received 27 July 2016; Accepted 4 March 2017

ABSTRACT

A graphene oxide-chitosan composite (GO-CS) adsorbent was synthesized, in which GO played a cross-linking role. The synthesized GO-CS had good acid-resistance and mechanical strength, which was attributed to excellent cross-linking. The GO-OS was evaluated as an adsorbent for the removal of Cr(VI) from aqueous solutions. Experimental results confirmed that GO-CS has an excellent adsorption capacity for Cr(VI) (~67.8 mg/g). Kinetic regression results showed that the adsorption kinetics were more accurately represented by a pseudo second-order model. The overall adsorption process was jointly controlled by external mass transfer and intra-particle diffusion, whereby intra-particle diffusion played a dominant role. The Langmuir isotherm model provided a good fit for the adsorption process. The remarkable adsorption capacity of the GO-CS for Cr(VI) can be attributed to the combined adsorption interaction mechanisms onto the GO-CS. The results of this work are significant for environmental applications of GO-CS as a promising adsorbent for the removal of heavy metal pollutants from aqueous solutions.

Keywords: Graphene; Cross-linking agent; Cr (VI); Adsorption; Acid-resisting

1. Introduction

Industrial wastewaters are a major concern for the government and public due to the emission of various organic pollutants and heavy metal contaminants. Among the heavy metal contaminants in wastewaters, chromium, especially Cr(VI), has received more attention because of its high toxicity and threat to human health [1,2]. Effluent concentrations can vary from tens to hundreds of milligrams/liter, and the USEPA has set a standard of 0.05 mg/l for the discharge of Cr(VI) to surface water, whereas total Cr is regulated to below a level of 2 mg/l [3]. Therefore, treatment of chromium-containing industrial effluent to meet government requirements and to protect the public is urgently needed. Among the different physicochemical treatments used for wastewater treatment, the adsorption technique has been a very effective method because of its low cost, easy operation and high efficiency, compared with other methods [4–6].

Chitosan (CS) is a linear natural polysaccharide that is composed of glucosamine and N-acetyl glucosamine units linked by a β-(1–4)-glycosidic bond [7]. Chitosan has attracted attention because of its excellent biocompatibility, hypotoxicity, antimicrobial activity and biodegradability [8–10]. Generally, CS has been widely used in tissue engineering, separation membranes, wound dressing, drug delivery and packaging materials [11]. CS can also be used as an adsorbent to remove heavy metals and dyes due to its active amino and hydroxyl groups [12]. However, the strong hydrogen bonds between the abundant amino and hydroxyl groups in CS create intrinsic

*Corresponding authors.

drawbacks, such as low mechanical properties and poor stability in acid media. To enhance the mechanical and anti-acid properties of CS-based materials, researchers have developed many effective modification strategies [13]. Cross-linking is a simple modification approach and can take place between CS and multi-functional anhydride or aldehyde reagents [14]. The cross-linking reagents that are traditionally used include organic solvents such as anhydride or aldehyde. However, during the cross-linking reaction, the volatile organic substance can be harmful to the environment and humans. Moreover, operation and implementation of the cross-linking reaction can be complicated. Therefore, green cross-linking methods for the operating procedure that are concise, easy, and have no harmful odor need to be developed.

Graphene, a single layer of carbon atoms in a hexagonal lattice, has recently attracted much attention due to its novel electronic and mechanical properties [15]. Graphene oxide (GO) is a typical pseudo-two-dimensional oxygen-containing solid in bulk form that possesses multiple functional groups, including hydroxyls, epoxides, and carboxyls [16–18]. GO has been used as a filler for the next generation of nanocomposite materials. However, there are few studies of the preparation of a supramolecular hydrogel using GO as a 2D cross-linker [19,20].

The large number of amino groups bonding onto the matrix of CS make CS an alkaline polysaccharide polymer; thus, the amino groups exhibit certain alkaline and nucleophilic properties [20]. By contrast, GO has certain acidic and carbenium ion characteristics [7], and GO contains hydroxyls, epoxides, and carboxyls. CS and GO are both high molecular weight polymers. When they are mixed together under certain conditions, they can react and produce new substances. The highly active epoxy group on the surface of GO can rapidly react with the amino group on the surface of CS via catalysis with a weak acid (carboxyl group) and weak base (amino-group) [21].

In this paper, a graphene oxide-chitosan composite (GO-CS) adsorbent was successfully synthesized, in which GO played a cross-linking role for the reaction between CS and GO. This synthesis method possessed the following advantages: (a) a low temperature, (b) the use of a non-organic solvent, and (c) a concise and easy operating procedure with no harmful odor. The resulting GO-CS was used as an adsorbent to remove Cr(VI) from an aqueous solution, and the composite exhibited an excellent adsorption capacity.

2. Materials and methods

2.1. Materials and chemicals

All chemicals were purchased from Sinopharm Chemical Reagent Co., Ltd (Shanghai, China) and were of analytical purity and used in the experiments directly without any further purification. All solutions were prepared using deionized water.

2.2. Preparation of GO-CS

The graphite oxide was prepared using a modified Hummer's method [22,23]. Graphite oxide was dispersed in deionized water and sonicated in an ultrasonic bath for 12 h. The sonicated dispersion was centrifuged for 20 min at 4000 rpm (revolutions per minute) to remove the unexfoliated graphite oxide particles from the supernatant. The obtained suspension of GO was then processed by freeze-drying the supernatant to obtain a GO powder. Chitosan (100 mg) was slowly added to a solution containing 200 mg of GO and the mixture was aggressively stirred for 10 min. The above-mentioned raw mixture was placed in an electric-heated thermostatic water bath at 80°C for 5 h. The raw product was filtered and freeze dried, and thus GO-CS was successfully created.

2.3. Batch adsorption experiments

Sorption isotherms were obtained using a batch equilibration technique. Solid-to-solution ratios were adjusted to obtain a 20–60% solute uptake by the sorbents. The solid-to-solution ratios used for the sorption of Cr(VI) by GO, CS and GO-CS were 0.2 mg/ml, 0.4 mg/ml and 0.6 mg/ml, respectively. A labeled stock solution of Cr(VI) was prepared with a buffer solution to maintain a pH of 2. Test solutions of Cr(VI) concentrations were prepared by introducing diphenylcarbazide into the buffer solution with Cr(VI) (GB7467-87). When the Cr(VI) had completely reacted with diphenylcarbazide, the absorbance value at 540 nm on a UV visible spectrophotometer (Techcomp UV2310 II) was monitored. A calibration curve of the relationship between the Cr(VI) concentrations and absorbance values was confirmed. The Cr(VI) concentrations in the solution were obtained based on the calibration curve. The total chromium concentration in the solution was obtained using an inductively coupled plasma emission spectrometer (ICP, Agilent 720ES, Japan).

Batch adsorption experiments were performed as follows: 10 mg of the adsorbent was introduced into a 25 ml conical flask containing 10 ml of Cr(VI) solution ranging from 5 mg/L to 33 mg/L. The flasks were sealed and shaken in a TS-2102C model Shaken Incubator shaker at a preset temperature at 120 rpm for 24 h to ensure adsorption equilibrium. The Cr(VI) uptake was calculated by conducting a mass balance before and after adsorption using the following equation:

$$Q_e = \frac{(C_0 - C_e) \times V_1}{W} \quad (1)$$

where V_1 (L) is the volume of the solution, W (g) is the mass of a given dry adsorbent, and C_0 and C_e (mg/L) are the initial and equilibrium concentrations, respectively, of Cr(VI) in the aqueous solution. For the kinetic study, the amount of adsorbent and solution were 200 mg and 200 ml, respectively, and 0.50 ml of the solution was sampled at various time intervals to determine the adsorption kinetics.

2.4. Characterization methods

The surface morphologies of the samples were visualized using a field-emission scanning electron microscope (SEM, Hitachi S-4800) operating at a typical accelerating voltage of 10 kV. Infrared spectra (FTIR) were obtained

using a Bruker FT-IR spectrometer (Bruker, Germany). To determine the functional groups and related oxidation states on the surface of the materials, X-ray photoelectron spectroscopy (XPS) analysis was carried out in a Kratos Axis Ultra DLD spectrometer with monochromatic Al/Ka X-rays at a base pressure of 1×10^{-9} Torr.

3. Results and discussion

3.1. Characterization of adsorbent

A powdery or bulk morphology was observed for the chitosan, as shown in Fig. 1a, whereas GO exhibited a schistose shape (Fig. 1b). When GO reacted with chitosan, a curved surface and laminated structure was observed (Fig. 1c, 1d). The curved surface and laminated structure of GO-CS is better for the adsorption of Cr(VI) from aqueous solutions.

As seen in Fig. 2, GO presented a strong peak at ~3300 cm^{-1}, which was attributed to hydroxyl groups, and there was another peak at 1250 cm^{-1}, which was attributed to ester groups. There were also peaks at ~1700 cm^{-1}, which were attributed to carbonyl groups. The above-mentioned results demonstrated that the surface of GO was decorated with carboxylic acid and hydroxyl and carbonyl groups. After GO reacted with chitosan, the characteristic peak from ester groups disappeared, and the characteristic peak intensity of the hydroxyl and carbonyl groups that bonded to the GO were weakened. The characteristic peaks at 3200 cm^{-1} (N-H) and 1100 cm^{-1} (C-N) were weakened and even disappeared.

As seen in Fig. 3a, the C1s binding energies of GO were 284.6 eV (C-C/C=C bond), 286.4 eV (C=O bond), and 287 eV (C-O/O-C=O bond). The C1s binding energies of GO-CS were 283.1 eV (C-C bond), 284.4 eV (C-O bond) and 285.5 eV (O-C=O bond) (Fig. 3b). After GO reacted with CS, the C-C binding energies of GO decreased by ~1.5 eV, the C-O binding energies of GO decreased by ~2 eV, and the O-C=O binding energies of GO decreased by ~1.5 eV, which further demonstrated that GO-CS was synthesized through the covalent cross-linking between GO and CS [24,25].

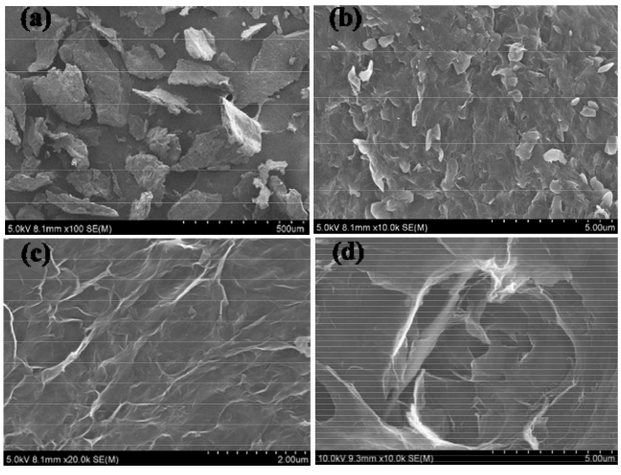

Fig. 1. SEM images of CS (a), GO (b) and GO-CS (c,d).

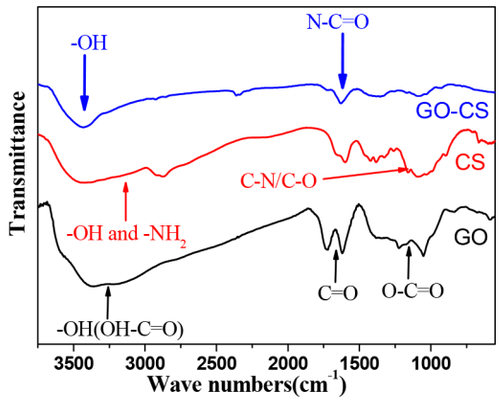

Fig. 2. IR spectrum of GO, CS and GO-CS.

As seen from Fig. 3c and 3d, the N1s binding energies of CS were ~397.9 eV (C-N bond), and the N1s binding energies of GO-CS were ~397.5 eV(C-N bond) and ~399.3 eV (N-C=O bond). These phenomena were attributed to the change in the nitrogen surroundings, which was attributed to the mutual reaction between GO and CS. Nitrogen in CS was in the amine form, whereas nitrogen in GO-CS was in the amide form. The above-mentioned results from XPS and IR spectra clearly demonstrate that GO had reacted with CS by covalent cross-linking. Two possible reaction mechanism are possible as follows: a) the opening cycle of the epoxy group can react with active hydrogen from the hydroxyl and amino functional group, and b) the carbonium of the carbonyl group can attack the active hydrogen from the hydroxyl and amino functional groups and produce new ester or amide groups [26,27].

3.2. Removal properties of Cr(VI)

As shown in Fig. 4a, no more than ~1% of the Cr(III) was detected during GO and GO-CS adsorption process within 1 h, which further demonstrated that reduction could not happen during the Cr(VI) removal process [28,29]. The Cr(VI) removal rate by GO-CS was stronger than that of GO, which was attributed to the better network structure that was formed between GO and CS. Table 1 present a comparison of the maximum adsorption capacities of Cr(VI) between our GO-CS and other adsorbents obtained from the literature. It is can be clearly seen that GO-CS had a excellent adsorption capacity as compared to other adsorbents.

These results indicated that GO and GO-CS exhibited different adsorption capacities for Cr(VI). The Cr(VI) removal ratio of GO-CS reached approximately 40%, whereas the Cr(VI) removal ratio of GO reached approximately 6% within 1 h. The outermost electron configuration of Cr(VI) was $3d^0 4s^0$, which left five 3d vacant orbitals and one 4s vacant orbital. Therefore, only when Cr(VI) formed six coordination bonds with six pairs of lone electrons could Cr(VI) be removed from the solution. Because GO-CS had more lone pair electrons than GO, the GO-CS can form more coordination bonds with Cr(VI) than GO. Moreover, GO-CS exhibited stronger Cr(VI) removal capacities than GO from the aqueous solution [36,37].

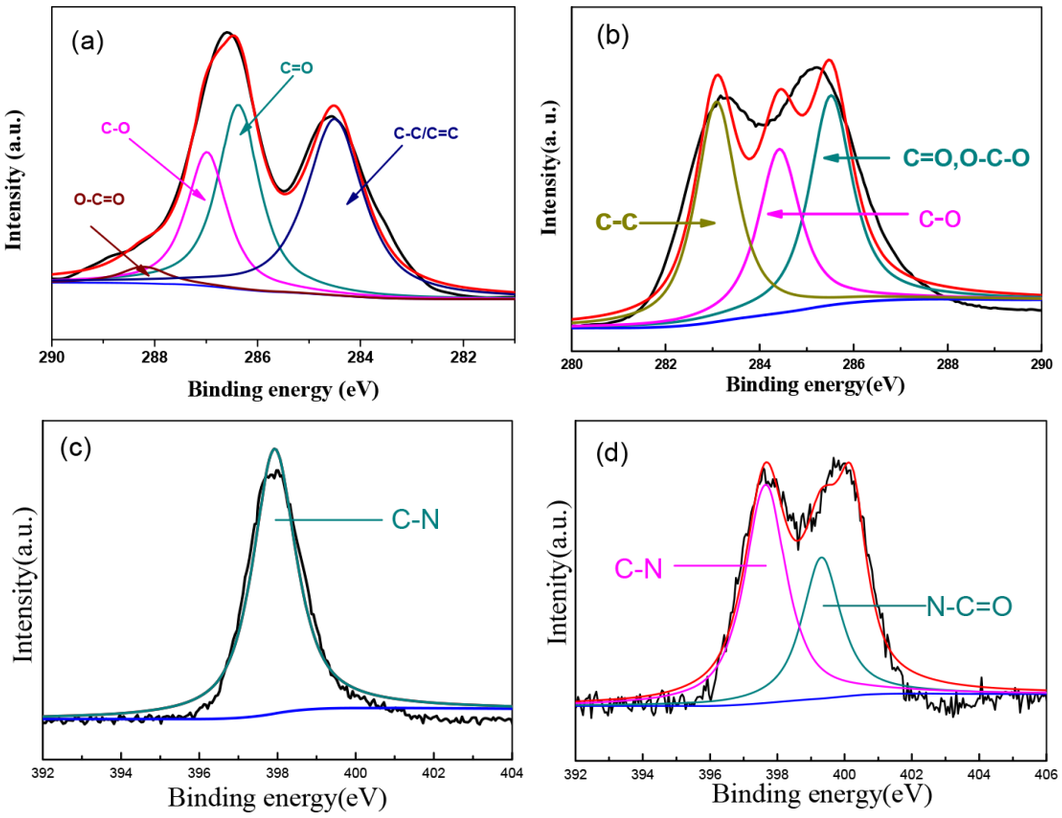

Fig. 3. C1s deconvolution of GO (a) and GO-CS (b) and N1s deconvolution of CS (c) and GO-CS (d).

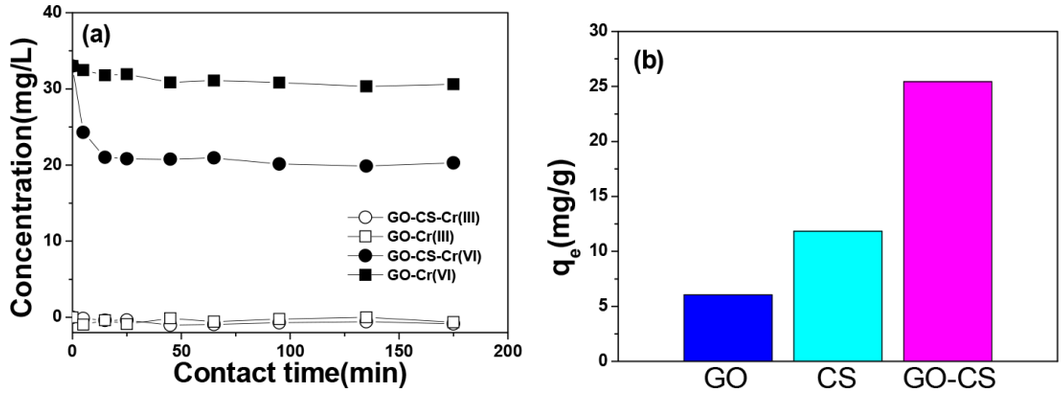

Fig. 4 (a). Cr(VI) or Cr(III) removal rates of GO and GO-CS (initial concentration = 33 mg/L, pH = 2). (b) Comparison of the Cr(VI) adsorption rates of GO and GO-CS.

Fig. 4b shows that the adsorption capacities of GO, CS and GO-CS for Cr(VI) were 7, 12.5 and 27.13 mg/g, respectively. The high Cr(VI) adsorption capacity of GO-CS was mainly attributed to GO-CS being able to form sufficient coordination bonds with the vacant orbitals located in the Cr(VI) matrix. These functional groups with many lone pair electrons can play a vital role during the adsorption process. The results of the adsorption capacities of GO-CS compared with GO and CS are as follows: the adsorption capacity of GO-CS increased by ~3.88 times compared with the adsorption of Cr(VI) by GO, and by ~2.17 times compared with the adsorption by CS.

3.3. Adsorption kinetics

Adsorption is a physicochemical process that involves the mass transfer of a substance from the liquid phase to the adsorbent surface; in this study, the adorption process involves Cr(VI) forming complexes with the hydroxyl groups on the GO-CS composite. An initial concentration of 33 mg/L for the corresponding Cr(VI) solution was utilized to investigate the adsorption kinetics of Cr(VI) on GO and GO-CS. The adsorption removal of Cr(VI) by GO-CS was rapid and reached equilibrium in ~20 min. The concentration gradients gradually reduced due to the accumulation

Table 1
Comparison of the adsorption capacities of Cr(VI) onto various adsorbents

Adsorbents	Adsorption capacity (mg/g)	Reference
IL-functionalized oxi-MWCNTs	85.83	[30]
Coconut tree sawdust	3.46	[31]
Porous Fe_3O_4 hollow microspheres/graphene oxide composite	32.33	[32]
Groundnut husk	7.0	[33]
SWCNTs	20.3	[34]
GO-CS	67.8	This work

of Cr(VI) adsorbing onto the surface sites of GO-CS, leading to the decline in the adsorption rate at a later stage. By contrast, the adsorption removal of Cr(VI) by GO was slow and reached equilibrium in ~50 min. More equilibrium time was required for the adsorption of Cr(VI) onto GO than onto GO-CS, which may be attributed to the different mechanisms of Cr(VI) adsorption onto GO and GO-CS (discussed in the subsequent sections).

The transient behavior of the Cr(VI) adsorption process was further investigated using three kinetic models: pseudo-first-order (PF), pseudo-second-order (PS) and the Weber-Morris model [38–40], which originated from chemical reaction kinetics. The constants k_1 (min^{-1}), k_2 (min^{-1}) and K_i are the pseudo-first order, pseudo-second order and Weber-Morris model adsorption rate constants, respectively; $q_{e,cal}$ (mg mg^{-1}) and C (mg mg^{-1}) are the sorption capacity at equilibrium and at time t, respectively.

The calculated kinetic parameters are presented in Table 2. By comparing the correlation coefficients (R^2), the Cr(VI) adsorption process onto GO and GO-CS was best described by the pseudo-second order model. The higher adsorption rate constant, k_2, of Cr(VI) onto GO-CS compared with Cr(VI) onto GO indicated a higher rate of Cr(VI) removal by GO-CS, which was consistent with the experimental data. Moreover, the calculated q values ($q_{e,cal}$) from the pseudo-second order model were much closer to the experimental data than those calculated from the pseudo-first order model.

Because the general kinetic analysis could not identify the rate-limiting step of the Cr(VI) adsorption process onto GO-CS and GO, an intra-particle diffusion model proposed by Weber and Morris was used. Plots of q_t vs. $t^{1/2}$ for Cr(VI) adsorption onto GO-CS and GO are shown in Fig. 5d. If the plots of q_t vs. $t^{1/2}$ yield a straight line and pass through the origin, the intra-particle diffusion would be the sole rate-limiting step in the entire adsorption process.

As shown in Fig. 5d, the adsorption plots of GO-CS and GO for Cr(VI) removal are non-linear over the entire time range, and the plots do not pass through the origin, indicating that intra-particle diffusion was involved but was not the rate-limiting step. If the data showed multi-linear stages, then two or more steps influenced the adsorption process, such as external diffusion and intra-particle diffusion. The result indicated that three steps existed in the entire adsorption process: (i) the instantaneous adsorption or external surface adsorption, possibly including the boundary layer diffusion of the solute molecules; (ii) the gradual adsorption stage, where intra-particle diffusion into mesopores and micropores was the rate-controlling step; and (iii) the final stage, where intra-particle diffusion started to slow down due to the relatively low residual Cr(VI) concentration in the solution.

The equilibrium adsorption capacities of Cr(VI) onto GO and GO-CS were 5.73 and 26 mg/g, respectively. The results indicated that GO-CS exhibited better adsorption performance than GO, which was ascribed to GO-CS containing more lone pair electrons than GO. Generally the removal rate of Cr(VI) is initially rapid but gradually decreases with time until it reaches equilibrium. This phenomenon was ascribed to the fact that a large number of vacant adsorption sites were available for adsorption at the initial stage and the remaining vacant adsorption sites gradually decreased with time.

3.4. Adsorption isotherms

Langmuir, Freundlich and Dubinin-Radushkevich (D-R) isotherm models [41] were used to fit the experimental data. The parameters obtained from nonlinear regression by the three models are listed in Fig. 6. The determination coefficients (R^2) of the Langmuir, Freundlich and D-R isotherms of GO-CS are summarized Table S2. Based on the determination coefficients shown in Table S2, the Langmuir isotherm model was a better fit for the adsorption data than the Freundlich isotherm model. The applicability of the Langmuir isotherm model suggested that the same sites with several adsorption energies were involved, and, in some cases,

Table 2
Kinetic parameters of pseudo first- and second-order adsorption kinetic models and Weber-Morris model for Cr(VI) on GO-CS or GO. (Cr(VI) concentration = 33 mg/L, GO-CS or GO = 0.33 g/L)

Adsorbents	Initial conc.	$q_{e,exp}$	Pseudo first-order model			Pseudo second-order model			Weber-Morris model		
	(mg/L)	(mg/g)	k_1 (min^{-1})	$q_{e,cal}$ (mg/g)	R^2	k_2 (min^{-1})	$q_{e,cal}$ (mg/g)	R^2	K_i (g·mg^{-1}·$min^{-0.5}$)	C (mg/g)	R^2
GO-CS	33	26.28	0.015	2.13	0.547	0.017	26.0	0.999	0.535	19.93	0.546
GO	33	5.32	0.012	1.76	0.822	0.007	5.73	0.9695	0.355	0.84	0.843

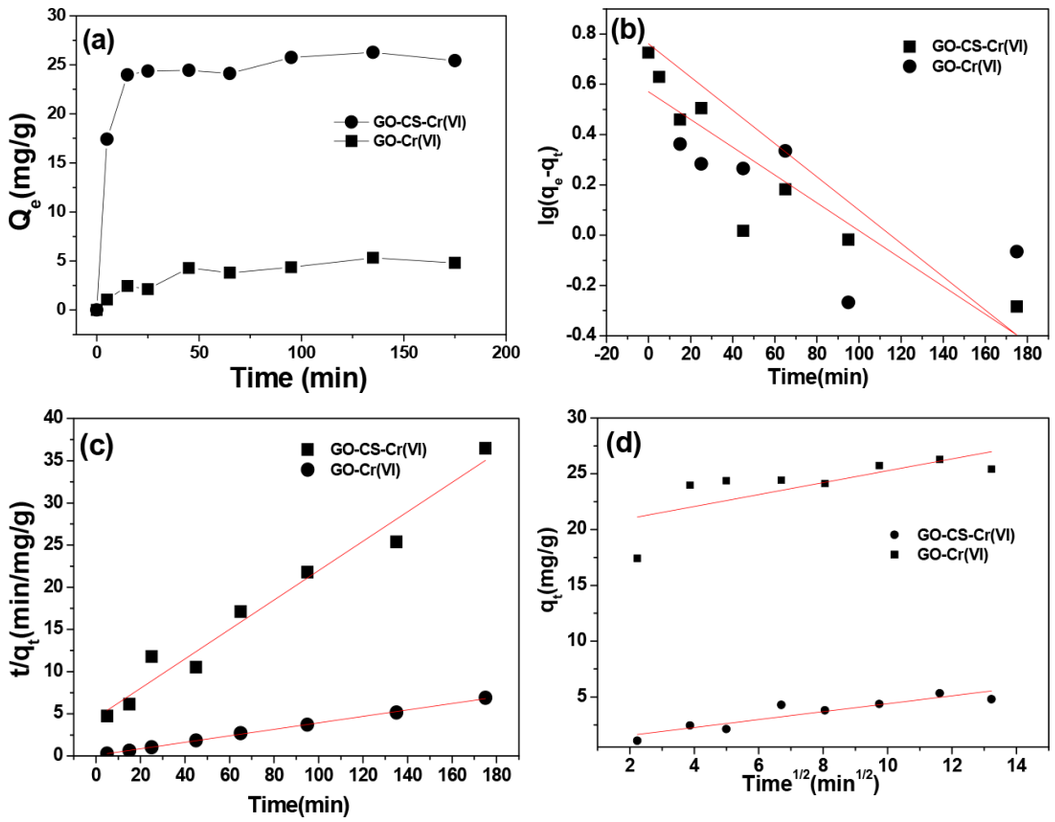

Fig. 5(a). Kinetic curves of Cr(VI) adsorption onto GO and GO-CS, (b) pseudo first-order model, (c) pseudo second-order model and (d) Weber-Morris model.

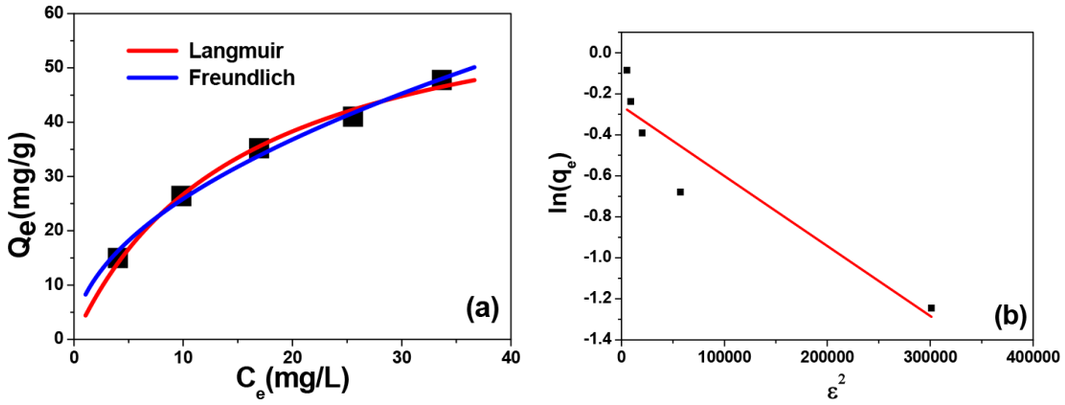

Fig. 6(a). Equilibrium adsorption isotherms and (b) D-R model of Cr(VI) onto GO-CS (Cr(VI) = 33 mg/L, GO-CS = 0.2 g/L).

the intermolecular interactions occurred between Cr(VI) and GO-CS. Table 3 shows that the computed maximum monolayer capacity was 26 mg/g for the adsorption of Cr(VI) onto GO-CS.

GO-CS exhibited stronger removal properties of Cr(VI) than traditional adsorbents, as shown in Table 3. GO-CS contains many nitrogen (amino) and oxygen (hydroxyl) with lone pair electrons, whereas the traditional adsorbents contain only a few oxygen groups. GO-CS can provide many electron pairs so that it can easily coordinate bonds with the vacant orbitals of Cr(VI) and therefore successfully remove Cr(VI) from aqueous solutions.

3.5. Effects of pH

The solution pH can affect the surface charge of the adsorbent, the radius of the chromium ions, and the dissociation of the functional groups on the active sites of the adsorbent [42]. Thus, the influence of pH on the removal

Table 3
Langmuir, Freundlich and Dubinin-Radushkevich isotherms parameters of GO-CS (Cr(VI) concentration = 33 mg/L, GO-CS: 0.2 g/L)

Absorbents	Langmuir model			Freundlich model			Dubinin-Radushkevich model			
	K_L(l/mg)	q_m(mg/g)	R^2	K_F	1/n	R^2	B (mol/kJ^2)	Q_m (mg/g)	E (kJ/mol)	R^2
GO-CS	0.065	67.8	0.992	7.996	0.510	0.991	3x10-13	40.1	1.3x106	0.886

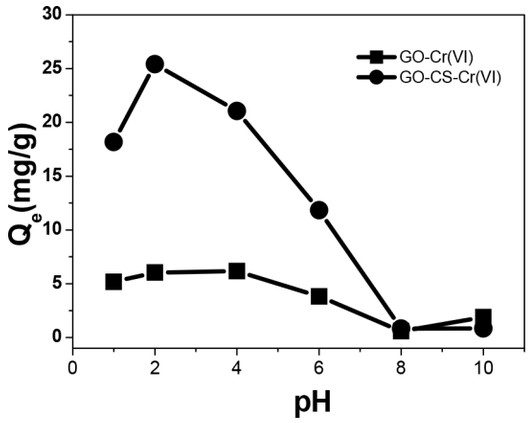

Fig. 7. Cr(VI) adsorption capacities onto GO and GO-CS at different pH values (Cr(VI) initial concentration = 33 mg/L, GO or GO-CS concentration = 0.33 mg/L).

of Cr(VI) by GO and GO-CS was studied to further investigate the adsorption process. The effect of the initial pH on the removal of Cr(VI) by GO and GO-CS is shown in Fig. 7. These results indicated that the removal of Cr(VI) by GO remained nearly constant over the pH range of 1–6, and decreased over the pH range of 6–10. When the pH value was between 1 and 6, GO exhibited weak and stable removal capacities of Cr(VI). When the pH value was above 6, the hydroxyl and carboxyl groups were gradually converted into anions; thus, the removal of Cr(VI) by GO decreased.

The effect of the initial pH on the removal of Cr(VI) by GO-CS is shown in Fig. 7. The Cr(VI) adsorption capacity onto GO-CS increased with increasing pH, and reached a maximum at a pH of 2. When the pH ranged from 2 to 8, the Cr(VI) adsorption capacity decreased and was stable and weak above a pH of 8.

When the pH value ranged from 1 to 2, the amide-functional group gradually increased as the pH value increased and then led to the increasing Cr(VI) adsorption capacity onto GO-CS. When the pH value was 2, the Cr(VI) adsorption capacity onto GO-CS was maximized; this was derived from the good and stable lattice-like structure in which sufficient Lewis bases from the nitrogen (amide and amino) and oxygen (hydroxyl, carboxyl) groups were available. When the pH value ranged from 2 to 8, the hydroxyl and carboxyl groups were converted into anions; thus, the Cr(VI) adsorption capacity onto GO-CS decreased to the same degree. When the pH value was above 8, because the amide group had slowly decomposed and the hydroxyl and carboxyl groups had been almost completely converted into anions, the Cr(VI) adsorption capacity became stable and negligible.

4. Conclusion

In summary, a graphene oxide-chitosan composite adsorbent was successfully synthesized, and GO played a cross-linking role for chitosan. The resulting GO-CS had good dispersion and many active oxygen-containing functional groups, which made GO-CS promising for use as an adsorbent for Cr(VI) removal from aqueous solutions. Indeed, GO-CS exhibited an excellent adsorption capacity and good acid-resisting properties. The results of this work are significant for environmental applications of GO-CS as a promising adsorbent material for the removal of heavy metal pollutants from aqueous solutions.

Acknowledgments

This research is supported by The National Natural Science Foundation of China (51408362, 21577099). We are also thankful to anonymous reviewers for their valuable comments that helped improve this manuscript.

References

[1] D.E. Kimbrough, Y. Cohen, A.M. Winer, L. Creelman, C. Mabuni, A critical assessment of chromium in the environment, Crit. Rev. Environ. Sci. Technol., 29 (1999) 1–46.
[2] A.L. Rowbotham, L.S. Levy, L.K. Shuker, Chromium in the environment: an evaluation of exposure of the UK general population and possible adverse health effects, J. Toxicol. Environ. Health-Part B-Crit. Revi., 3 (2000) 145–178.
[3] A. Baral, R.D. Engelken, Chromium-based regulations and greening in metal finishing industries in the USA, Environ. Sci. Policy, 5 (2002) 121–133.
[4] M. Dakiky, M. Khamis, A. Manassra, M. Mer'eb, Selective adsorption of chromium(VI) in industrial wastewater using low-cost abundantly available adsorbents, Adv. Environ. Res., 6 (2002) 533–540.
[5] D. Mohan, C.U. Pittman, Activated carbons and low cost adsorbents for remediation of tri- and hexavalent chromium from water, J. Hazard. Mater., 137 (2006) 762–811.
[6] M. Owlad, M.K. Aroua, W.A.W. Daud, S. Baroutian, Removal of hexavalent chromium-contaminated water and wastewater: a review, Water, Air, Soil Pollut., 200 (2009) 59–77.
[7] Y. Pan, H. Bao, L. Li, Noncovalently functionalized multiwalled carbon nanotubes by chitosan-grafted reduced graphene oxide and their synergistic reinforcing effects in chitosan films, ACS Appl. Mater. Interf., 3 (2011) 4819–4830.
[8] C.-K. Yao, J.-D. Liao, C.-W. Chung, W.-I. Sung, N.-J. Chang, Porous chitosan scaffold cross-linked by chemical and natural procedure applied to investigate cell regeneration, Appl. Surf. Sci., 262 (2012) 218–221.
[9] K. Lewandowska, Surface studies of microcrystalline chitosan/poly (vinyl alcohol) mixtures, Appl. Surf. Sci., 263 (2012) 115–123.
[10] F. Yu, L. Chen, J. Ma, Y. Sun, Q. Li, C. Li, M. Yang, J. Chen, Self-regenerative adsorbent based on the cross-linking chitosan for adsorbing and mineralizing azo dye, RSC Adv., 4 (2014) 5518–5523.

[11] T. Tojima, H. Katsura, M. Nishiki, N. Nishi, S. Tokura, N. Sakairi, Chitosan beads with pendant α-cyclodextrin: preparation and inclusion property to nitrophenolates, Carbohyd. Polym., 40 (1999) 17–22.
[12] F.C. Wu, R.L. Tseng, R.S. Juang, Enhanced abilities of highly swollen chitosan beads for color removal and tyrosinase immobilization, J. Hazard. Mater., 81 (2001) 167–177.
[13] F. Kara, E.A. Aksoy, Z. Yuksekdag, N. Hasirci, S. Aksoy, Synthesis and surface modification of polyurethanes with chitosan for antibacterial properties, Carbohyd. Polym., 112 (2014) 39–47.
[14] D. Li, M.B. Müller, S. Gilje, R.B. Kaner, G.G. Wallace, Processable aqueous dispersions of graphene nanosheets, Nature Nanotech., 3 (2008) 101–105.
[15] J.L. Vickery, A.J. Patil, S. Mann, Fabrication of graphene–polymer nanocomposites with higher-order three-dimensional architectures, Adv. Mater., 21 (2009) 2180–2184.
[16] Y. Xu, Q. Wu, Y. Sun, H. Bai, G. Shi, Three-dimensional self-assembly of graphene oxide and DNA into multifunctional hydrogels, ACS Nano, 4 (2010) 7358–7362.
[17] H. Bai, C. Li, X. Wang, G. Shi, A pH-sensitive graphene oxide composite hydrogel, Chem. Commun., 46 (2010) 2376–2378.
[18] F. Yu, Y. Li, S. Han, J. Ma, Adsorptive removal of antibiotics from aqueous solution using carbon materials, Chemosphere, 153 (2016) 365–385.
[19] T. Mita, J. Chen, Y. Sato, Synthesis of arylglycines from CO_2 through α-amino organomanganese species, Organic Lett., 16 (2014) 2200–2203.
[20] Y.H. Jhon, J.-G. Shim, J.-H. Kim, J.H. Lee, K.-R. Jang, J. Kim, Nucleophilicity and accessibility calculations of alkanolamines: applications to carbon dioxide absorption reactions, J. Phys. Chem., A, 114 (2010) 12907–12913.
[21] Y. Song, H. Liu, H. Tan, F. Xu, J. Jia, L. Zhang, Z. Li, L. Wang, pH-switchable electrochemical sensing platform based on chitosan-reduced graphene oxide/concanavalin a layer for assay of glucose and urea, Anal. Chem., 86 (2014) 1980–1987.
[22] J. Ma, C. Li, F. Yu, J. Chen, "Brick-like" N-doped graphene/carbon nanotube structure forming three-dimensional films as high performance metal-free counter electrodes in dye-sensitized solar cells, J. Power Sources, 273 (2015) 1048–1055.
[23] W.S. Hummers Jr, R.E. Offeman, Preparation of graphitic oxide, J. Amer. Chem. Soc., 80 (1958) 1339–1339.
[24] E.Y. Polyakova, K.T. Rim, D. Eom, K. Douglass, R.L. Opila, T.F. Heinz, A.V. Teplyakov, G.W. Flynn, Scanning tunneling microscopy and X-ray photoelectron spectroscopy studies of graphene films prepared by sonication-assisted dispersion, ACS Nano, 5 (2011) 6102–6108.
[25] C.D. Zangmeister, Preparation and evaluation of graphite oxide reduced at 220C, Chem. Mater., 22 (2010) 5625–5629.
[26] H.J. Martin, K.H. Schulz, J.D. Bumgardner, K.B. Walters, XPS study on the use of 3-aminopropyltriethoxysilane to bond chitosan to a titanium surface, Langmuir, 23 (2007) 6645–6651.
[27] G. Lawrie, I. Keen, B. Drew, A. Chandler-Temple, L. Rintoul, P. Fredericks, L. Grøndahl, Interactions between alginate and chitosan biopolymers characterized using FTIR and XPS, Biomacromolecules, 8 (2007) 2533–2541.
[28] A. Lu, S. Zhong, J. Chen, J. Shi, J. Tang, X. Lu, Removal of Cr (VI) and Cr (III) from aqueous solutions and industrial wastewaters by natural clino-pyrrhotite, Environ. Sci. Technol., 40 (2006) 3064–3069.
[29] A. Carnizello, L. Marçal, P. Calefi, E. Nassar, K. Ciuffi, R. Trujillano, M. Vicente, S. Korili, A. Gil, Takovite–aluminosilicate nanocomposite as adsorbent for removal of Cr (III) and Pb (II) from aqueous solutions, J. Chem. Eng. Data, 54 (2008) 241–247.
[30] A.S.K. Kumar, S.J. Jiang, W.L. Tseng, Effective adsorption of chromium(VI)/Cr(III) from aqueous solution using ionic liquid functionalized multiwalled carbon nanotubes as a super sorbent, J. Mater. Chem. A, 3 (2015) 7044–7057.
[31] K. Selvi, S. Pattabhi, K. Kadirvelu, Removal of Cr (VI) from aqueous solution by adsorption onto activated carbon, Bioresour. Technol., 80 (2001) 87–89.
[32] M.C. Liu, T. Wen, X.L. Wu, C.L. Chen, J. Hu, J. Li, X.K. Wang, Synthesis of porous Fe_3O_4 hollow microspheres/graphene oxide composite for Cr(VI) removal, Dalton T, 42 (2013) 14710–14717.
[33] S.P. Dubey, K. Gopal, Adsorption of chromium (VI) on low cost adsorbents derived from agricultural waste material: a comparative study, J. Hazard. Mater., 145 (2007) 465–470.
[34] C. Jung, J. Heo, J. Han, N. Her, S.J. Lee, J. Oh, J. Ryu, Y. Yoon, Hexavalent chromium removal by various adsorbents: Powdered activated carbon, chitosan, and single/multi-walled carbon nanotubes, Sep. Purif. Technol., 106 (2013) 63–71.
[35] J. Hu, C.L. Chen, X.X. Zhu, X.K. Wang, Removal of chromium from aqueous solution by using oxidized multiwalled carbon nanotubes, J. Hazard Mater., 162 (2009) 1542–1550.
[36] P. Luo, J.-s. Zhang, B. Zhang, J.-h. Wang, Y.-f. Zhao, J.-d. Liu, Preparation and characterization of silane coupling agent modified halloysite for Cr (VI) removal, Indust. Eng. Chem. Res., 50 (2011) 10246–10252.
[37] Y. Xu, J. Zhang, G. Qian, Z. Ren, Z.P. Xu, Y. Wu, Q. Liu, S. Qiao, Effective Cr (VI) removal from simulated groundwater through the hydrotalcite-derived adsorbent, Indust. Eng. Chem. Res., 49 (2010) 2752–2758.
[38] R.M. Tinnacher, P.S. Nico, J.A. Davis, B.D. Honeyman, Effects of fulvic acid on Uranium (VI) sorption kinetics, Environ. Sci. Technol., 47 (2013) 6214–6222.
[39] P.F. Salipante, S.D. Hudson, A colloid model system for interfacial sorption kinetics, Langmuir (2015).
[40] F. Yu, S. Sun, S. Han, J. Zheng, J. Ma, Adsorption removal of ciprofloxacin by multi-walled carbon nanotubes with different oxygen contents from aqueous solutions, Chem. Eng., J. 285 (2016) 588–595.
[41] G. Bronner, K.-U. Goss, Sorption of organic chemicals to soil organic matter: influence of soil variability and pH dependence, Environ. Sci. Technol., 45 (2010) 1307–1312.
[42] H. Shen, J. Chen, H. Dai, L. Wang, M. Hu, Q. Xia, New insights into the sorption and detoxification of chromium (VI) by tetraethylenepentamine functionalized nanosized magnetic polymer adsorbents: mechanism and pH effect, Indust. Eng. Chem. Res., 52 (2013) 12723–12732.